Heart Rate Variability Monitoring Using a Wearable Armband

Jesús Lázaro[1,2,3], Natasa Reljin[1], Yeonsik Noh[4], Pablo Laguna[2,3], Ki H Chon[1]

[1] Department of Biomedical Engineering, University of Connecticut, Storrs CT, USA
[2] BSICoS Group, Aragón Institute for Engineering Research (I3A), IIS Aragón, University of Zaragoza, Zaragoza, Spain
[3] CIBER in Bioengineering, Biomaterials and Nanomedicine (CIBER-BBN), Madrid, Spain
[4] College of Nursing and Department of Electrical and Computer Engineering, University of Massachusetts, Amherst, MA, USA

Abstract

A wearable electrocardiogram (ECG) monitor is evaluated as heart rate variability (HRV) monitor. The device consists of an armband designed to be worn on the left upper arm which provides 3 ECG channels based on 3 pairs of dry (no hydrogel) electrodes. Armband-ECG and conventional-Holter-ECG signals were simultaneously recorded from 14 subjects during 5 minutes in supine position. Spacial principal component analysis was used to obtain a unique armband ECG signal in which the electromyogram contribution is attenuated. QRS complexes were automatically detected. Five traditional HRV parameters were derived: SDNN, RMSSD, pNN50, and powers within low frequency (LF, [0.04, 0.15] Hz) and high frequency (HF, [0.15, 0.4] Hz) bands. The Pearson's correlation coefficient between the measurements from the armband device and the measures from the Holter device was computed. Results show very high correlations (1.0000, 0.9999, 0.9984, 1.0000, and 0.9999 for SDNN, RMSSD, pNN50, and powers at LF and HF, respectively), suggesting that the quality of armband-ECG signals is enough to estimate HRV parameters during stationary movement restricted conditions.

1. Introduction

Continuous monitoring of heart beat occurrences has a wide range of applications, such as atrial fibrillation detection [1]. The heart beat occurrences can be used to derive the heart rate and its variability (HRV), extending the range of applications including, *e.g.*, epileptic seizures detection [2], and stress level monitoring [3]. In fact, HRV remains a powerful framework for non-invasive assessment of the autonomic nervous system (ANS) [4] which has been studied in a large number of applications in the last decades. Continuous electrocardiogram (ECG) monitoring is usually performed by using Holter monitors, which are not convenient for a long-term daily monitoring because they use uncomfortable obstructive leads, and wet electrodes over the chest that cause skin irritation after few days.

Aiming to overcome the above mentioned limitations of the conventional Holter devices, a wearable armband device for ECG monitoring is being developed in our lab at the University of Connecticut. This armband records three ECG channels using three pairs of hydrophobic dry electrodes [5], differentially, while it is being worn in the left upper arm. This armband device is more convenient for daily long-term recordings than conventional Holter monitors, since it causes no skin irritation and uses no leads. However, using dry electrodes over the left upper arm represents a more challenging setup than the conventional Holter setup, which is based on wet electrodes over the chest. The armband setup relies on electrodes that are placed very close to each other over main limb muscles which usually generate powerful electromyogram signals, specifically from biceps and triceps. Furthermore, although these electrodes have a good impedance matching with the skin considering that they are dry electrodes, the impedance matching of hydrogel wet electrodes is better.

Nevertheless, a pilot study suggested that the armband device provides ECG signals with enough quality to obtain a QRS-morphology-based respiratory rate estimation during laboratory-controlled movement restricted conditions [6]. Complementing a continuous respiratory rate monitoring with a heart rate and HRV monitoring would extend the range of applications including sleep studies [7], and it would allow to improve a stress level estimation [8]. However, the armband device has been not been evaluated as a HRV monitor. In this paper, a first approach to evaluate the armband device as a HRV monitor is presented.

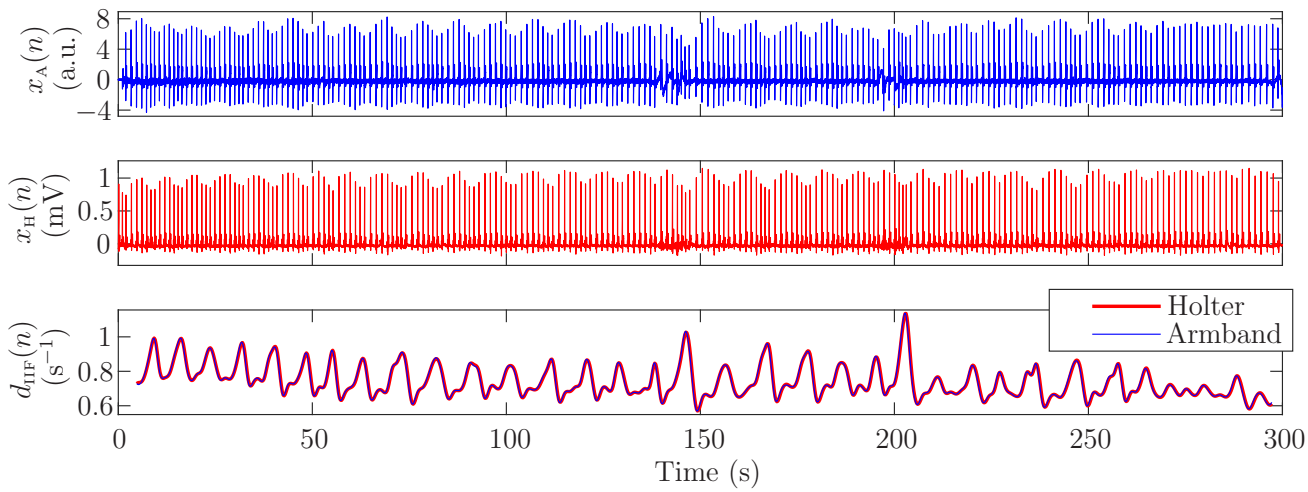

Figure 1: Example of first principal component of the 3 armband ECG channels ($x_A(n)$), Holter ECG channel ($x_H(n)$), and their associated inverse interval functions ($d_{IIF}(n)$).

2. Methods

2.1. Data and signal preprocessing

The three armband-ECG signals were recorded from 14 subjects (10 male) during 5 minutes in supine position. The armband was worn on the left upper arm and uses a sampling rate of 1000 Hz. In order to have a reference, an additional ECG signal was simultaneously recorded by a Rozinn RZ 153+ (Glendale, NY, USA) Holter device available in the market. Three ECG channels were recorded by this Holter device using a sampling rate of 180 Hz.

All ECG signals were resampled to $F_s = 250$ Hz. The sampling rate is a trade-off situation. The higher sampling rate the higher computational cost and battery consumption, while the lower sampling rate the lower time resolution. The value of 250 Hz was chosen because it is the minimum recommended for calculating the classical HRV indices [4]. Then, baseline was attenuated by a high-pass filter with a cut-off frequency of 0.3 Hz, and power line was attenuated by a non-linear technique described in [9].

A spatial principal component analysis (PCA) was performed, and the first principal component was chosen as the unique armband-ECG signal for further analysis. The reason of this choice is that this first principal component is expected to have an attenuated contribution of the electromyogram from the local muscles (mainly left biceps and triceps) [10]. This signal is denoted $x_A(n)$ in this paper. In parallel, a unique ECG channel was visually chosen from the Holter device for each subject, based on the observed signal-to-noise ratio. This signal is denoted $x_H(n)$ in this paper. An example of these signals can be observed in Fig. 1.

2.2. Heart rate variability analysis

QRS complexes were automatically detected by an algorithm based on the variable frequency complex demodulation described in [11], and normal beats (n_{N_i}) were determined by the algorithm presented in [12]. Then, the inverse interval function was computed as:

$$d^u_{IIF}(n) = \sum_i \frac{1}{n_{N_i} - n_{N_{i-1}}} F_s \delta(n - n_{N_i}), \qquad (1)$$

where the superscript "u" denotes that the signal is unevenly sampled, as the normal beats occur non uniformly in time. An evenly-sampled version of $d^u_{IIF}(n)$ was obtained by cubic splines interpolation using a sampling rate of 4 Hz, and it is denoted $d_{IIF}(n)$ in this paper.

Two inverse interval functions were obtained: one from $x_A(n)$, and another one from $x_H(n)$. As $x_A(n)$ and $x_H(n)$ are obtained from two independent devices, they are not synchronized in time. In order to synchronize them, their relative delay was estimated from the cross correlation between their associated inverse interval functions computed from the segment of 2 minutes occurring at the center of the 5 analyzed minutes. The delay was estimated as that lag at which the cross correlation is maximum, and then, it was corrected accordingly.

Once the delay was corrected, the normal-beat-to-normal-beat (NN) intervals were computed, and the following time-based HRV parameters were estimated as recommended in [4]:

- SDNN: Standard deviation of NN intervals during the 5 minutes.
- RMSSD: Root mean square of the successive differences of NN intervals during the 5 minutes.

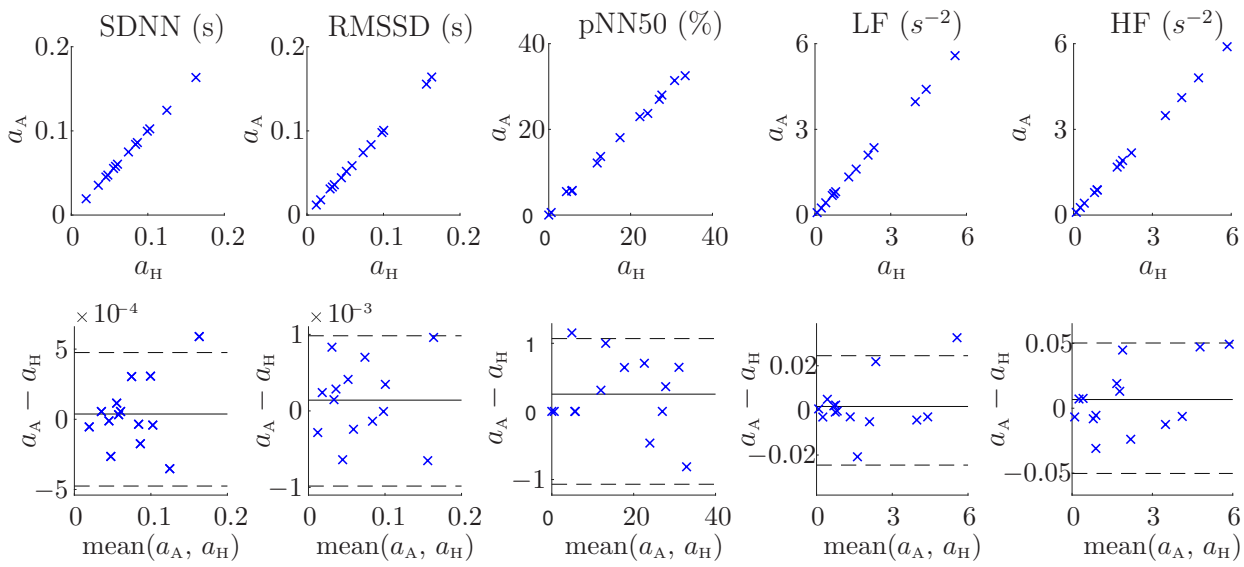

Figure 2: Scatterplots of HRV parameters estimated from the armband (a_A) versus those estimated from the Holter device (a_H) (first row), and the corresponding Bland-Altman plots (second row).

• pNN50: The proportion of pairs of successive NN intervals that differ by more than 50 ms during the 5 minutes.

Subsequently, the power spectral density of $d_{IIF}(n)$ was estimated by using the Welch Periodogram with a 1-minute-length Hamming window and 50% of overlap. Then, the powers within low frequency (LF, [0.04, 0.15] Hz) and at high frequency (HF, [0.15, 0.4] Hz) were computed by integrating this power spectral density within the corresponding bands.

Additionally, the same HRV parameters (SDNN, RMSSD, pNN50, and powers at LF and HF bands) were computed also from $x_H(n)$ for using them as reference.

For each one of the studied HRV parameters, two estimations per subject were available: one from the armband and one from the Holter. The Pearson's correlation coefficient ρ between the two devices was computed. In addition, the corresponding Bland-Altman plots were also computed.

3. Results

Scatterplots of HRV parameters estimated from the armband versus those estimated from the Holter device are shown in Fig. 2. Additionally, the corresponding Bland-Altman plots are also shown. Table 1 shows the obtained Person's correlation coefficients, and the limits of agreement (LOA) obtained from the Bland-Altman plots.

4. Discussion

A wearable armband device which records ECG signals has been evaluated as a HRV monitor during laboratory-controlled no-movement conditions. The armband is worn on the left upper arm and it incorporates three pairs of dry (no hydrogel) electrodes which are used differentially to record three ECG channels. The armband is much more convenient than a Holter device for long-term monitoring because it causes no skin irritation and it uses no obstructive leads. PCA was used to derive a unique armband ECG channel in which the electromyogram component is attenuated. A conventional Holter device available in the market was used as reference.

QRS complexes were automatically detected and 5 classical HRV parameters were computed from them: SDNN, RMSSD, pNN50, and powers at LF and HF bands. In order to evaluate the agreement of the HRV parameters measured from the armband with those measured from the Holter device, the inter-subject Pearson's correlation coefficient was computed, and the corresponding scatterplots and Bland-

Table 1: Obtained inter-subject Pearson's correlation (ρ) coefficients between HRV parameters estimated from the armband and those estimated from the Holter. In addition, the limits of agreement (LOA) obtained from the corresponding Bland-Altman plots are also shown.

	ρ	LOA (mean $\pm$ 1.96$\times$SD)
SDNN	1.0000	3.76E-5 $\pm$ 4.75E-4 s
RMSSD	0.9999	1.41E-4 $\pm$ 9.82E-4 s
pNN50	0.9984	2.53E-1 $\pm$ 1.07 %
LF	1.0000	1.75E-3 $\pm$ 2.45E-2 s^{-2}
HF	0.9999	6.72E-3 $\pm$ 5.03E-2 s^{-2}

Altman plots were performed.

Scatterplots show a clear linear relation between the HRV parameters measured from the armband and those measured from the Holter (see Fig. 2). This linear relation is quantified by the obtained Pearson's correlation coefficients which were very close to 1 for the 5 studied HRV parameters (see Table 1), demonstrating a very high positive correlation. Furthermore, the limits of agreement obtained from the Bland-Altman plots were at least one order of magnitude lower than their mean value for the 5 studied HRV parameters.

These results suggest that there is an excellent agreement between the HRV parameters measured from the armband and those measured from the the Holter. Thus these results indicate that the armband device is potentially useful for certain applications such as stress level assessment [8] and sleep studies [13]. However, the analysis performed in this study is limited to healthy volunteers in laboratory-controlled movement restricted conditions. Future studies are needed in order to evaluate the armband as a HRV monitor in specific applications, *e.g.*, during daily life for long-term monitoring applications such as stress level assessment, or during polysomnography for sleep studies.

5. Conclusions

Results suggest that the armband device can substitute a Holter device for HRV monitoring during movement restricted conditions. Future studies have to be elaborated to assess the performance of the armband in specific applications.

Acknowledgements

This project has received funding from the European Union's Framework Programme for Research and Innovation Horizon 2020 (2014-2020) under the Marie Skłodowska-Curie Grant Agreement No. 745755. This work was supported also by Gobierno de Aragón (Reference Group BSICoS T39-17R) cofunded by FEDER 2014-2020 "Building Europe from Aragon", and by CIBER in Bioengineering, Biomaterials & Nanomedicine (CIBER-BBN) through Instituto de Salud Carlos III. This work was also supported by NSF SBIR Phase I (#1746589) and R43 HL135961.

References

[1] Dash S, Chon KH, Lu S, Raeder EA. Automatic real time detection of atrial fibrillation. Annals of Biomedical Engineering 2009;37(9):1701–1709.

[2] Zijlmans M, Flanagan D, Gotman J. Heart rate changes and ECG abnormalities during epileptic seizures: prevalence and definition of an objective clinical sign. Epilepsia 2002;43(8):847–854.

[3] Castaldo R, Montesinos L, Melillo P, James C, Pecchia L. A novel algorithm for the automatic detection of sleep apnea from single-lead ECG. BMC Medical Informatics and Decision Making 2019;19(1).

[4] Task Force of the European Society of Cardiology and the North American Society of Pacing and Electrophysiology. Heart rate variability: standards of measurement, physiological interpretation and clinical use. Circulation 1996; 93(5):1043–1065.

[5] Reyes BA, Posada-Quintero HP, Bales JR, Clement AL, Pins GD, Swiston A, Riistama J, Florian JP, Shykoff B, Qin M, Chon KH. Novel electrodes for underwater ECG monitoring. IEEE Transactions on Biomedical Engineering 2014;61:1863–1876.

[6] Lázaro J, Bailón R, Gil E, Noh Y, Laguna P, Chon KH. Pilot study on electrocardiogram derived respiratory rate using a wearable armband. In XLV International Conference on Computing in Cardiology. 2018; 1–4.

[7] de Chazal P, Heneghan C, Sheridan E, Reilly R, Nolan P, O'Malley M. Automated processing of the single-lead electrocardiogram for the detection of obstructive sleep apnoea. IEEE Transactions on Biomedical Engineering 2003; 50(6):686–696.

[8] Hernando A, Lázaro J, Gil E, Arza A, Garzón JM, López-Antón R, de la Cámara C, Laguna P, Aguiló J, Bailón R. Inclusion of respiratory frequency information in heart rate variability analysis for stress assessment. IEEE Journal of Biomedical and Health Informatics 2016;20(4):1016–1025.

[9] Sörnmo L, Laguna P. ECG signal processing. In Bioelectrical Signal Processing in Cardiac and Neurological Applications. Elsevier, 2005; 473–484.

[10] Castells F, Laguna P, Sörnmo L, Bollmann A, Roig JM. Principal component analysis in ECG signal processing. IEURASIP Journal on Advances in Signal Processing 2007; 2007(1):074580.

[11] Bashar SK, Noh Y, Walkey AJ, McManus DD, Chon KH. Verb: Vfcdm-based electrocardiogram reconstruction and beat detection algorithm. IEEE Access 2019;7:13856–13866.

[12] Mateo J, Laguna P. Analysis of heart rate variability in presence of ectopic beats using the heart timing signal. IEEE Transactions on Biomedical Engineering 2003;50(3):334–343.

[13] Varon C, Caicedo A, Testelmans D, Buyse B, Van Huffel S. A novel algorithm for the automatic detection of sleep apnea from single-lead ECG. IEEE Transactions on Biomedical Engineering 2015;62(9):2269–2278.

Address for correspondence:

Jesús Lázaro
Department of Biomedical Engineering, UCONN
260 Gleenbrook Rd, Unit 3247, 06269 Storrs CT, USA
jesus.lazaro@uconn.edu